

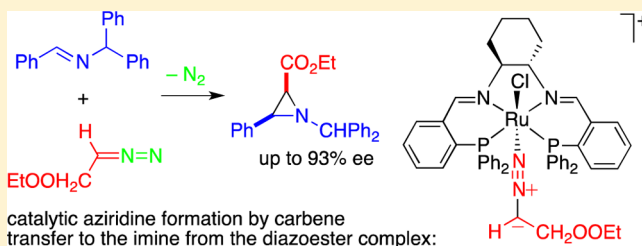
Highly Enantioselective Ruthenium/PNNP-Catalyzed Imine Aziridination: Evidence of Carbene Transfer from a Diazoester Complex

Joël Egloff, Marco Ranocchiari, Amata Schira, Christoph Schotes, and Antonio Mezzetti*

Department of Chemistry and Applied Biosciences, ETH Zürich, CH-8093 Zürich, Switzerland

S Supporting Information

ABSTRACT: The ruthenium/PNNP complexes $[\text{RuCl}(\text{Et}_2\text{O})(\text{PNNP})]\text{Y}$ ($\text{Y} = \text{PF}_6, 4\text{PF}_6; \text{BF}_4, 4\text{BF}_4$; or $\text{SbF}_6, 4\text{SbF}_6$) (10 mol %) catalyze the enantioselective aziridination of imines with ethyl diazoacetate (EDA) as carbene source (PNNP = (1*S*,2*S*)-*N,N'*-bis[*o*-(diphenylphosphino)-benzylidene]cyclohexane-1,2-diamine). The highest enantioselectivity was obtained with 4SbF_6 , which aziridinated *N*-benzylidene-1,1-diphenylmethanamine (**5a**) to *cis*-ethyl 1-benzhydryl-3-phenylaziridine-2-carboxylate (*cis*-**6a**) with 93% ee at 0 °C. To the best of our knowledge, this is the highest enantioselectivity ever obtained in transition metal-catalyzed asymmetric aziridination. Aziridine yields were overall moderate to low (up to 33% isolated yield of the *cis* isomer) because of the competitive formation of diethyl maleate (**7**). The scope of the catalyst was studied with *p*- and *m*-substituted imines. NMR spectroscopic studies with ^{13}C - and ^{15}N -labeled EDA indicate that aziridine **6a** is formed by carbene transfer from an EDA complex, $[\text{RuCl}(\text{EDA})(\text{PNNP})]\text{PF}_6$ (**8**), to the imine. The observation of a dinitrogen complex (**9**) gives further support to this mechanism. The EDA adduct **8** decomposes to the carbene complex $[\text{RuCl}(\text{CHCO}_2\text{Et})(\text{PNNP})]^+$ (**10**), whose reaction with EDA gives diethyl maleate. This unprecedented mechanism is rationalized on the basis of the nucleophilic nature of diazoalkanes, which is enhanced by coordination to a π -back-donating metal such as ruthenium(II).



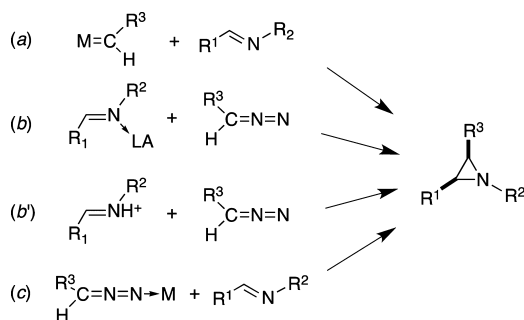
INTRODUCTION

Chiral alkoxy carbonyl-substituted aziridines are valuable strain-activated electrophilic precursors to amino acids as they undergo ring-opening with excellent stereo- and regiocontrol.¹ A straightforward approach to their synthesis is the catalytic aziridination² of aldimines with diazo compounds.³ During the last 20 years, this transformation has been performed with catalysts that involve an intermediate carbene complex (Scheme 1a) or, alternatively, Lewis (or Brønsted) acid activation of the imine (Scheme 1b or 1b').

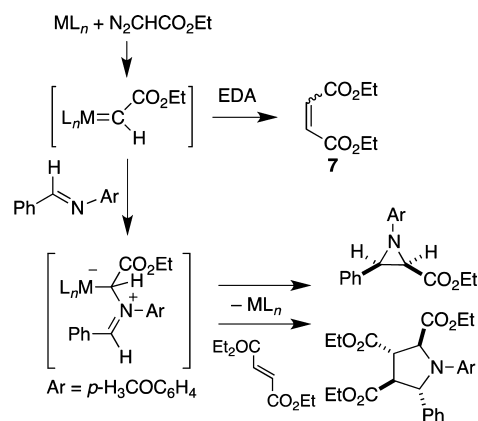
In 1995, Jacobsen reported copper bisoxazoline catalysts that operate by nucleophilic attack of the imine onto a carbene

complex formed from ethyl diazoacetate (EDA) (Scheme 1a).⁴ He suggested that the resulting nitrogen ylide is relatively stable and can partially dissociate from the chiral catalyst before collapsing to aziridine, as indicated by the formation of pyrrolidines in the presence of dimethyl fumarate (Scheme 2). This broadly supported mechanism⁵ explains the low enantioselectivity typically observed both with copper catalysts

Scheme 1



Scheme 2



Received: July 25, 2013

Published: August 14, 2013

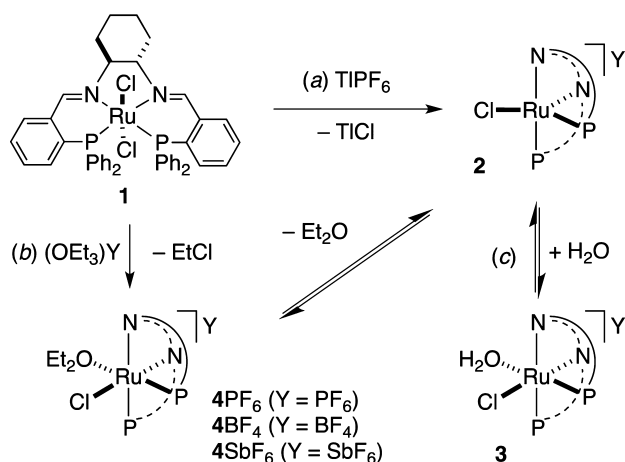


and with rhodium(II) catalysts⁶ and has contributed to the reputation of transition metal-catalyzed imine aziridination as a reaction of intrinsically low enantioselectivity ever since.

Other copper catalysts that possibly involve Lewis acid activation of the imine showed improved enantioselectivity, but their performance was still modest.⁷ A successful variation of the carbene transfer approach combines a metal catalyst for diazoester decomposition with a chiral sulfide that acts as carbene shuttle to imine via a sulfur ylide intermediate,⁸ but the source of the chiral information is not the metal in this case. The alternative approach in metal-catalyzed aziridination, that is, nitrene transfer to an olefin,⁹ has been pioneered by Evans and Jacobsen and further developed by Katsuki with the use of sulfonyl azides.¹⁰ Following seminal work with achiral systems,¹¹ chiral, boron-based Lewis acids have been successfully used for asymmetric imine aziridination.¹² More recently, chiral Brønsted acids have been shown to induce the aza-Darzens reaction of imines and diazoalkanes with high enantioselectivity.^{13–15} In both cases, the reaction mechanism involves the nucleophilic attack of the diazoester onto the acid-activated imine (Scheme 1, pathways b and b'). Driven by the success of this approach, the mechanistic understanding of acid-catalyzed imine aziridination has been rapidly evolving. Thus, it has been recently shown that, in the VAPOL-catalyzed aziridination, the imine is activated by hydrogen bonding to a chiral Brønsted acid derived from the chiral borane.^{12b}

Our interest in carbene transfer to imines arises from previous studies of asymmetric cyclopropanation with ruthenium complexes containing chiral tetradentate PNNP ligands such as (1*S*,2*S*)-*N,N'*-bis[*o*-(diphenylphosphino)-benzylidene]cyclohexane-1,2-diamine, which is used throughout this paper. The five-coordinate complex [RuCl(PNNP)]PF₆ (**2**), formed by chloride abstraction from [RuCl₂(PNNP)] (**1**) (Scheme 3),^{16,17} is a highly enantioselective catalyst for the

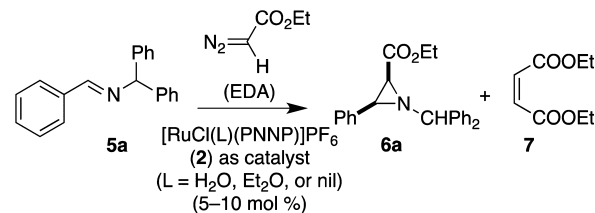
Scheme 3



asymmetric, *cis*-selective cyclopropanation of olefins by diazoesters with the intermediacy of the carbene complex [RuCl(CHCO₂Et)(PNNP)]⁺.¹⁸ Therefore, on the basis of the dominant mechanistic hypothesis, it was straightforward to test Ru/PNNP catalysts in imine aziridination with ethyl diazoacetate (EDA) (Scheme 4).

We have recently reported a preliminary screening of the Ru/PNNP catalysts [RuCl(L)(PNNP)]PF₆ (L = nil; **2**; L = OH₂, **3**; L = Et₂O, **4PF₆**),¹⁹ which showed that the Et₂O adduct **4PF₆** aziridates *N*-benzylidene-1,1-diphenylmethanamine

Scheme 4



(**5a**) to *cis*-ethyl 1-benzhydryl-3-phenylaziridine-2-carboxylate (*cis*-**6a**) with good enantioselectivity (up to 84% ee).²⁰ Maleate formation severely reduced the yield of aziridine, which was optimized by using a temperature gradient between −78 °C and room temperature. An NMR study gave strong evidence that aziridine is formed by carbene transfer to the imine from a coordinated diazoester molecule (Scheme 1c), an unprecedented mechanism that opens the way to highly enantioselective transition metal-catalyzed imine aziridination. In the present paper, we report further advances in terms of chemo- and enantioselectivity and substrate scope achieved by tuning the counterion Y[−] of the catalyst [RuCl(OEt₂)(PNNP)]Y (**4Y**; Y = PF₆, BF₄, or SbF₆), give a full account of the previously communicated NMR spectroscopic studies,²⁰ and suggest a general explanation for the reactivity of carbene and diazoester complexes with imines.

RESULTS AND DISCUSSION

Counterion Optimization and Substrate Scope. As mentioned above, the catalyst [RuCl(OEt₂)(PNNP)]PF₆ (**4PF₆**) gave significant yield of *cis*-ethyl 1-benzhydryl-3-phenylaziridine-2-carboxylate (*cis*-**6a**) only in combination with an elaborate temperature protocol.^{20,21} With the goal of producing aziridine in reasonable yield and high enantioselectivity under simpler experimental conditions, the catalysts [RuCl(OEt₂)(PNNP)]Y (**4Y**) containing other low-coordinating anions Y (Y = BF₄[−] or SbF₆[−]) were screened with *N*-benzylidene-1,1-diphenylmethanamine (**5a**) as standard substrate (Table 1).

The dichloro complex [RuCl₂(PNNP)] (**1**) was activated with (OEt₃)Y (Y = BF₄ or SbF₆, 1 equiv) overnight in dichloromethane to give **4Y** (Scheme 3), after which **5a** and then EDA were added to the solution cooled at 0 °C. The

Table 1. Asymmetric Aziridination of **5a** (at 0 °C) with Precatalyst **1** Activated with (OEt₃)Y^a

entry	Y	EDA (equiv)	crude 6 ^b		isolated <i>cis</i> - 6	
			yield (%)	<i>cis:trans</i>	yield ^c (%)	ee ^d (%)
1	PF ₆	1	22	77:23	13	80
2	BF ₄	1	32	78:22	24	78
3	SbF ₆	1	32	85:15	24	93
4	PF ₆	4	35	79:21	30	53 ^e
5	BF ₄	4	53	81:19	20	78
6	SbF ₆	4	58	78:22	40	67

^aReaction conditions: EDA (0.48 mmol, 1 equiv vs **5a**) was added (neat) in one portion to a CH₂Cl₂ solution (3 mL) containing imine **5a** (0.48 mmol) and **4Y** (10 mol %), prepared by activation of [RuCl₂(PNNP)] (**1**) (0.048 mmol) with (Et₃O)Y (0.048 mmol) overnight. The total reaction time was 24 h at 0 °C. ^bSum of *cis* and *trans* isomers, based on the imine, by ¹H NMR spectroscopy. ^cIsolated yield. ^dThe absolute configuration of *cis*-**6a** was 2*R*,3*R*. ^eThe isolated aziridine was contaminated with variable amounts of diethyl maleate.

reaction of 4PF_6 at a constant temperature of 0°C gave aziridine *cis*-**6a** in low isolated yield (13%) and 80% ee (entry 1). The tetrafluoroborate analogue 4BF_4 gave *cis*-**6a** with higher yield (24%), but with lower enantioselectivity (78% ee, entry 2). Finally, with the hexafluoroantimonate analogue 4SbF_6 , *cis*-**6a** was isolated with 24% yield and 93% ee (entry 3), which is, to the best of our knowledge, the highest enantioselectivity ever achieved in transition metal-catalyzed imine aziridination.

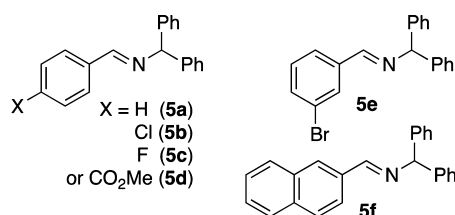
Major amounts of diethyl maleate (**7**) were formed with all catalysts, as usually observed in imine aziridination with carbenoids.⁴ Furthermore, variable amounts of the *trans*-aziridine (*trans*-**6a**) were detected in the crude reaction mixture.²² This is in contrast with the previously reported preliminary experiments with 4PF_6 as catalyst, in which no more than trace amounts of the *trans* isomer were formed in the reaction run between -78°C and room temperature.²⁰ However, even when *trans*-aziridine was clearly visible in the ^1H NMR spectrum of the crude products, pure *cis*-**6a** was readily isolated after workup (mostly as a crystalline solid), as the *trans* isomer was eluted together with the unreacted imine **5a**.²³

In an attempt to improve the yield of aziridine, an excess of EDA (4 equiv) was used with catalysts **4Y** (entries 4–6). Overall, lower enantioselectivity was achieved under these conditions, and large amounts of diethyl maleate (**7**) were formed, which hindered the purification of **6a** and other selected aziridines (see Supporting Information, Table S1). Overall, the best results were obtained with catalyst 4SbF_6 in combination with a stoichiometric amount of EDA. Therefore, these conditions were used to screen the substrate scope (see below).

At this stage, we do not have an explanation for the anion effect, in particular on the enantioselectivity. Low-temperature ^{31}P and ^{19}F NMR spectroscopic studies of the Et_2O adducts $[\text{RuCl}(\text{OEt}_2)(\text{PNNP})]\text{Y}$ (**4Y**, $\text{Y} = \text{PF}_6$, BF_4 , or SbF_6) in CD_2Cl_2 aimed at detecting possible cation/anion interactions showed that the dissociation of the Et_2O adduct **4** into the five-coordinate complex **2** and Et_2O is the main dynamic process in solution and failed to give conclusive evidence of the cation/anion interactions evoked by the counterion effect observed in catalysis (see Supporting Information). However, an interesting observation that will be discussed in the context of the general mechanism is that the yield of aziridine is higher with the SbF_6^- and BF_4^- counterions, which are more coordinating than PF_6^- .²⁴

The substituted benzaldimines **5b–5f** (Chart 1) were used to screen the scope of the reaction with complex 4SbF_6 as catalyst

Chart 1



(10 mol %) under the conditions used above for **5a** (1 equiv of EDA, CH_2Cl_2 , 0°C) (Table 2). The 4-(2-propyl)- and 4-methylphenyl analogues of **5a** gave lower chemo- and/or enantioselectivity and are not discussed further (see Supporting Information). Pure *cis*-aziridines **6b–6f** were obtained after workup as discussed above, and their absolute configuration

Table 2. Asymmetric Aziridination of Imines **5a–5f** with EDA Catalyzed by 4SbF_6 ^a

entry	imine	crude 6 ^b		isolated <i>cis</i> - 6	
		yield (%)	<i>cis:trans</i>	yield ^c (%)	ee ^d (%)
1	5a	32	85:15	24	93
2	5b	18	85:15	14	91
3	5c	16	84:16	9	75
4	5d	30	<i>cis</i> only	24	79
5	5e	46	93:7	34	83
6	5f	40	90:10	33	93

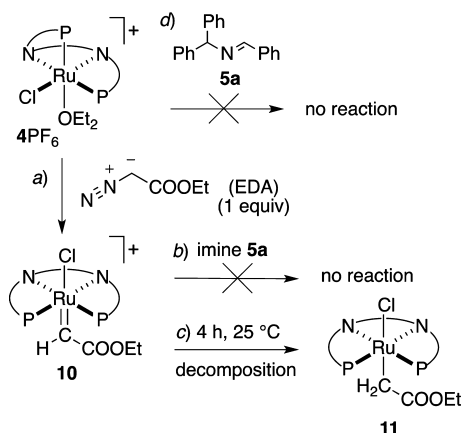
^aReaction conditions: See footnote a in Table 1. ^bSum of *cis* and *trans* isomers, based on the imine, by ^1H NMR spectroscopy. ^cIsolated yield of *cis*-aziridine. ^dThe absolute configuration of *cis*-**6a** was 2*R*,3*R*; those of **6b–6f** were not assigned.

was not determined. Besides **5a**, the catalyst 4SbF_6 gives enantioselectivity higher than 90% ee with the *p*-chloro- and 2-naphthyl-substituted imines **5b** and **5f** (91 and 93% ee, respectively, entries 2, 6). The 3-bromo analogue **5e** is formed with a slight erosion of enantioselectivity (83% ee), but with the highest isolated yield (34%, entry 5). The bulky 4-methoxycarbonyl-substituted imine **5d** gave the corresponding aziridine *cis*-**6d** with lower enantioselectivity (79% ee, entry 4), whereas 4-fluoro-substitution reduced both yield and enantioselectivity (entry 3). Interestingly, all these substrates gave higher enantioselectivity than obtained with other chiral transition metal catalysts that operate by diazoalkane activation.⁴

Finally, we note that the ^1H NMR spectra of the reaction crude of the catalytic runs reported in Tables 1 and 2 showed not more than trace amounts (<3% of starting imine) of enaminoesters (such as (*Z*)-ethyl 3-(benzhydrylamino)-3-phenylacrylate for imine **5a**, see Supporting Information). As enaminoesters are common byproducts with aziridination catalysts that operate by Lewis acid activation of the imine (path b in Scheme 1),¹¹ this observation disfavors such a reaction mechanism as discussed later on. The extended substrate scope and the improvement of yield and enantioselectivity achieved upon changing the counterion from PF_6^- to SbF_6^- show that the ruthenium/PNNP catalysts still have potential in asymmetric imine aziridination. This motivates us to report and discuss at full length the previously communicated¹⁹ stoichiometric and catalytic reactions between precatalyst 4PF_6 , EDA, and imine **5a** by NMR spectroscopy, because they are the key to the understanding and improvement of the chemoselectivity, which is the major issue at this juncture.

Attempted Carbene Transfer from $[\text{RuCl}(\text{CHCO}_2\text{Et})(\text{PNNP})]^+$ (10**).** As the literature precedents pointed to a carbene-mediated reaction, we studied first the reaction of imine **5a** with the previously reported^{18a,c} carbene complex $[\text{RuCl}(\text{CHCO}_2\text{Et})(\text{PNNP})]^+$ (**10**), which was prepared by adding EDA (1 equiv) to $[\text{RuCl}(\text{OEt}_2)(\text{PNNP})]\text{PF}_6$ (4PF_6) in CD_2Cl_2 at -78°C . Complex **10** was obtained as the main product (71%) (Scheme 5a), as indicated by the ^{31}P NMR spectrum of the reaction solution recorded at -78°C just thereafter, along with a small amount (15%) of a dinitrogen complex that we tentatively formulate as *trans*- $[\text{RuCl}(\text{N}_2)(\text{PNNP})]^+$ (**9**) (as suggested by the analogous reaction with $^{15}\text{NNCHCO}_2\text{Et}$, see below).²⁵ When imine **5a** (1 equiv) was added to this solution at -78°C , no spectral changes were observed. Therefore, the sample was slowly warmed to room

Scheme 5



temperature in 20 °C steps. A (¹³C,¹H)-HMQC experiment showed that no aziridine was formed (Scheme 5b).

After 4 h at room temperature, the reaction solution contained the alkyl complex *trans*-[RuCl(CH₂CO₂Et)-(PNNP)]⁺ (**11**) (43%) (Scheme 5c), along with the dinitrogen complex **9** (57%, see below). The alkyl complex **11** features two diagnostic doublets at δ 3.79 and 3.36 (²J_{H,H'} = 11.2 Hz) in the ¹H NMR spectrum, which were assigned to the diastereotopic H atoms of the Ru–CH₂CO₂Et moiety by means of (³¹P,¹H)-HMQC and (¹³C,¹H)-HMQC experiments. The ³¹P NMR spectrum of **11** is a tight AB pattern at δ 47.9 (d, J = 28.2 Hz) and 47.8 (d, J = 28.2 Hz) (202 MHz, CD₂Cl₂, 298 K, Figure S6 in the Supporting Information). Carbene complexes of Rh(III) and Co(III) porphyrins, formed by reaction with EDA, are known to give hydride abstraction from undefined sources, possibly EDA itself or the solvent, to give the corresponding alkyl complex.²⁶

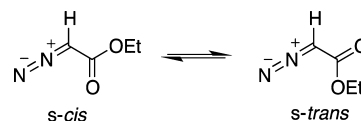
As the carbene complex **10** fails to transfer the carbene to imine **5a** and to give aziridine **6a**, we rule out that the aziridination reaction occurs according to path a in Scheme 1. To double-check the possible involvement of a carbene intermediate in catalytic aziridination, we used a standard trapping test for azomethine ylides.⁴ In a catalytic run performed with **4PF₆** as catalyst (10 mol %) and the temperature gradient described above in the presence of dimethyl fumarate (10 equiv vs **5a**), the aziridine yield was only slightly reduced from 26 to 23%, and no pyrrolidine was observed, which strongly disfavors the intermediacy of an azomethine ylide⁴ and, more in general, of a carbene complex (path a in Scheme 1).²⁷

Attempted Coordination of the Imine. In an experiment designed to test the alternative pathway involving Lewis acid activation of the imine (Scheme 1b), imine **5a** (1 equiv) was added to [RuCl(OEt₂)(PNNP)]⁺ (**4PF₆**) in CD₂Cl₂. As indicated by the ³¹P NMR spectra of the reaction solution at 25 and –78 °C, the main species present in solution is the unreacted complex **4PF₆**, and no signals were detected that may be assigned to an imine ruthenium complex (Scheme 5b).²⁸ Also, (³¹P,¹H)-HMQC and (¹H,¹H)-NOESY experiments at –78 °C showed that there is no significant contact between the H atoms of the PNNP ligand and those of imine **6a**, which further rules out the formation of an imine complex, at least in detectable amounts. The addition of EDA (1 equiv) to this solution at –78 °C converted **4PF₆** to the carbene complex **10**, which decomposed after several hours at room temperature without producing aziridine.

A New Mechanism for Carbene Transfer to Imine. The reactions discussed in the former two paragraphs rule out the classical mechanisms that have been proposed for carbene transfer to imines. The failure of carbene complex **10** to react with the imine (Scheme 5) and the ylide trapping test with fumarate rules out path a in Scheme 1. Lewis acid activation of the imine (path b) is excluded because we found no evidence of imine coordination by NMR spectroscopy, the presence of imine **5a** has no influence on the course of the reaction between **4PF₆** and EDA, and catalyst **4PF₆** produces only traces of enamino esters such as (Z)-ethyl 3-(benzhydrylamino)-3-phenylacrylate, which are typically formed in substantial amounts in Lewis acid catalyzed imine aziridination.¹¹ To overcome the impasse, we decided to study the aziridination reaction by NMR spectroscopy under conditions as close as possible to those of the catalytic reaction. To this goal, the reaction between EDA and imine **5a** in the presence of complex **4PF₆** was repeated with an excess of EDA. The experiments were carried out with isotope-labeled N₂¹³CHCO₂Et (¹³C-EDA) and with ¹⁵NNCHCO₂Et (¹⁵N-EDA) to enhance the sensitivity.

An excess of ¹³C-EDA (10 equiv) was added to [RuCl(OEt₂)(PNNP)]⁺ (**4PF₆**) and imine **5a** (1:1 ratio) in CD₂Cl₂ at –78 °C.²⁹ The (¹³C,¹H)-HMQC spectrum at this temperature showed that no aziridine had formed. The major ¹³C-labeled compound was unreacted ¹³C-EDA,³⁰ whose ¹³C NMR carbenoid signal is split because of slow interconversion between the *s-cis* and *s-trans* isomers (in ca. 1:1 ratio) (Scheme 6, Figure 1), which has been observed previously both for free³¹

Scheme 6



and for metal-bound ethyl diazoacetate.³² It should be noted that the low-temperature splitting affects all the ¹H, ¹³C, and ¹⁵N NMR signals of the N=N=CH–CO₂Et moiety, either free or metal-bound.

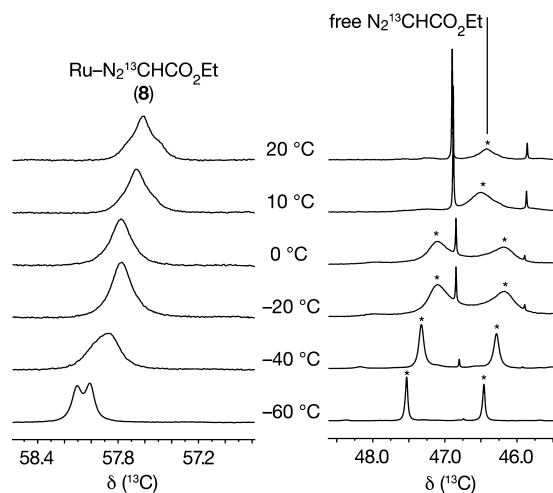
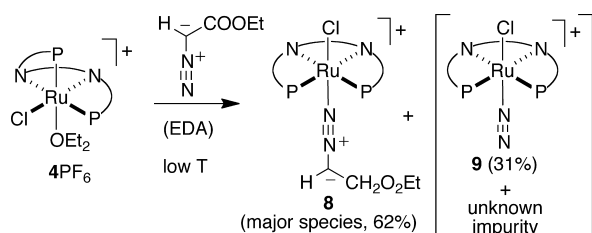


Figure 1. ¹³C NMR CHCO₂Et signals of complex ¹³C-**8** and of free EDA (marked with “*”) (126 MHz, CD₂Cl₂).

As no aziridine was observed at $-78\text{ }^{\circ}\text{C}$, the sample was slowly warmed to $-20\text{ }^{\circ}\text{C}$, at which temperature a small amount (10%) of ^{13}C -labeled aziridine was detected by means of a $(^{13}\text{C}, ^1\text{H})$ -HMQC experiment. After the sample was cooled to $-60\text{ }^{\circ}\text{C}$ to slow down the reaction, the ^{13}C , ^1H , ^{31}P (and ^{15}N , see below) NMR spectra revealed that the major species present in the reaction solution was the ethyl diazoester complex *trans*- $[\text{RuCl}(^{13}\text{C}\text{-EDA})(\text{PNNP})]^+$ (^{13}C -8) (Scheme 7).³³

Scheme 7



In the ^{13}C NMR spectrum, the carbenoid $\text{N}_2\text{CHCO}_2\text{Et}$ carbon atom of ^{13}C -8 resonates at δ 58.0 and 58.1, which is diagnostic of an approximately linear $\text{N}-\text{N}-\text{C}$ moiety³⁴ and close to that of the free diazoalkane at δ 47.5 and 46.5 (*s-cis* and *s-trans*, respectively) (Figure 2).^{31a} The ^{13}C (and ^1H) NMR

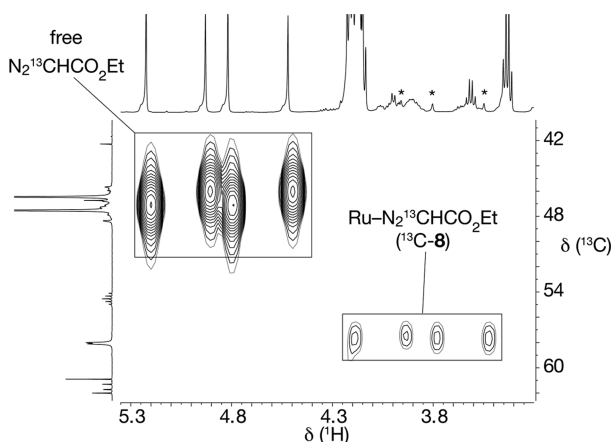


Figure 2. $(^{13}\text{C}, ^1\text{H})$ -HMQC NMR spectrum of the reaction solution of 4PF_6 , imine **5a**, and ^{13}C -EDA (1:1:10) (500 MHz, CD_2Cl_2 , $-60\text{ }^{\circ}\text{C}$). The CHCO_2Et signals of ^{13}C -8 are labeled “*”.

signals of ^{13}C -8 exhibit the typical dynamic behavior discussed above for ^{13}C -EDA (Figure 1), but the decoalescence temperature is much lower than for free EDA, which will be discussed below.

The ^{31}P NMR spectrum of the reaction solution at $-60\text{ }^{\circ}\text{C}$ (Figure 3) shows that the major P-containing species in solution is the ^{13}C -EDA complex ^{13}C -8 (62%), whose signals appear as two resolved AX systems (**8a** and **8b**) in a 1:1 ratio owing to the freezing out of the *s-cis*/*s-trans* isomerism. Besides the signals of the *s-cis* and *s-trans* isomers of EDA complex ^{13}C -8,³⁵ a slightly broadened signal at ca. δ 49 (31% of total intensity) is assigned to the dinitrogen complex **9** (Scheme 7). The AX patterns marked with asterisks in Figures 3 and 4 belong to the already observed noncarbenoid impurity (see footnote 28).

The assignment of signals **8a** and **8b** to the *s-cis* and *s-trans* rotamers of **8** in slow mutual exchange at this temperature was

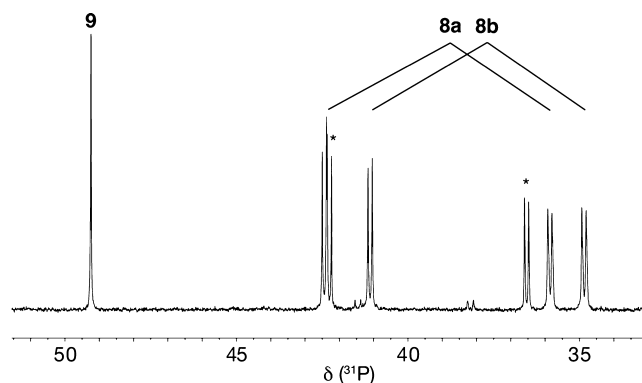


Figure 3. ^{31}P NMR spectrum (202 MHz, CD_2Cl_2 , $-60\text{ }^{\circ}\text{C}$) of the reaction solution of 4PF_6 with ^{13}C -EDA (10 equiv) showing the signals (**8a** and **8b**) of $[\text{RuCl}(^{13}\text{C}\text{-EDA})(\text{PNNP})]^+$ (^{13}C -8) (62%), dinitrogen complex **9** (29%), and of an unknown impurity (marked with an asterisk) (9%).

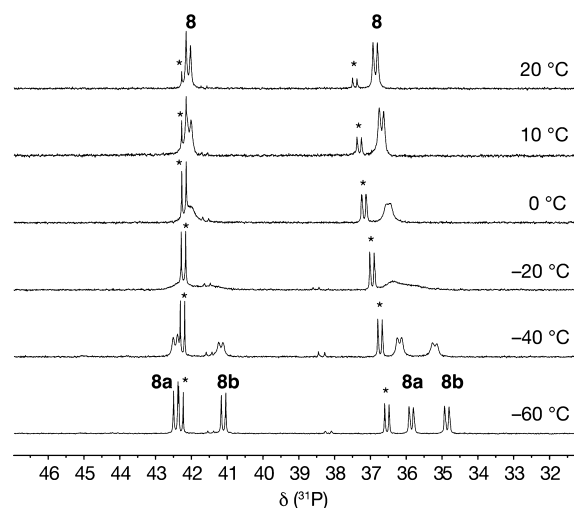
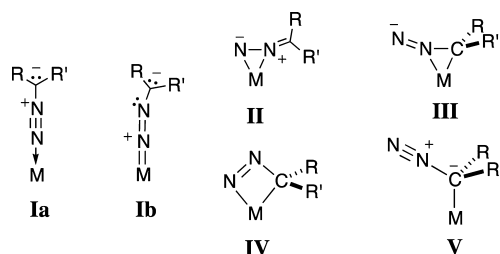


Figure 4. ^{31}P NMR signals of ^{13}C -8 (202 MHz, CD_2Cl_2) at different temperatures showing the decoalescence of the signals of the *s-cis* and *s-trans* isomers (**8a** and **8b**) (the asterisk marks the unknown impurity deriving from 4PF_6).^{25,28}

confirmed by a selective irradiation experiment of the ^{31}P NMR signal at δ 42.1 at $-40\text{ }^{\circ}\text{C}$, which saturated and suppressed the signal of the other isomer at δ 41.1. Accordingly, upon raising the temperature to $-20\text{ }^{\circ}\text{C}$, the signals coalesce and then resolve into a single AX system at $20\text{ }^{\circ}\text{C}$ (Figure 4). Finally, a $(^{31}\text{P}, ^1\text{H})$ -HMQC NMR spectrum at $-60\text{ }^{\circ}\text{C}$ (Figure S9 in the Supporting Information) revealed the signals of the $\text{N}_2^{13}\text{C}-\text{H}$ proton of the ^{13}C -EDA ligand, which does not exhibit NOESY contacts to any other signal.

We formulate the EDA complex *trans*- $[\text{RuCl}(\text{EDA})(\text{PNNP})]\text{PF}_6$ as an *end-on* diazoalkane complex of type **Ia** or **Ib** (Chart 2) on the basis of the ^{13}C NMR shifts and of chemical analogy, as transition metals of the d^6 configuration tend to form linear or singly bent *end-on* diazoalkane complexes.^{34a,36,37} For instance, $[\text{RuCl}_2(\text{L})(\text{PNP})]$ (L = diazofluorene, PNP = 2,6-bis(di-*tert*-butylphosphinomethyl)pyridine) features $\text{Ru}-\text{N}-\text{N}$ and $\text{N}-\text{N}-\text{C}$ angles of $158.3(2)^\circ$ and $170.1(3)^\circ$, respectively.^{34g} Linear *end-on* diazoalkane complexes are well-known with d^8 metals as well, and in particular of rhodium(I) and iridium(I).^{34d-f}

Chart 2



Conclusive evidence of the formation of the EDA (**8**) and dinitrogen (**9**) complexes was obtained by repeating the above reaction, *ceteris paribus*, with terminally ^{15}N -labeled $^{15}\text{NNCHCCOEt}$ (^{15}N -EDA, see Supporting Information). The ^{31}P NMR spectrum of the reaction solution at $-80\text{ }^{\circ}\text{C}$ shows a $^2J_{\text{P,N}}$ coupling constant of about 2 Hz in the high-frequency ^{31}P NMR signals of the *cis*- $\text{P}-\text{Ru}-^{15}\text{NNCHCCOEt}$ moiety of *trans*- $[\text{RuCl}(^{15}\text{N-EDA})(\text{PNNP})]^+$ ($^{15}\text{N-8}$) (Figure 5).³⁸ The ^{15}N NMR spectrum of the reaction solution at -60

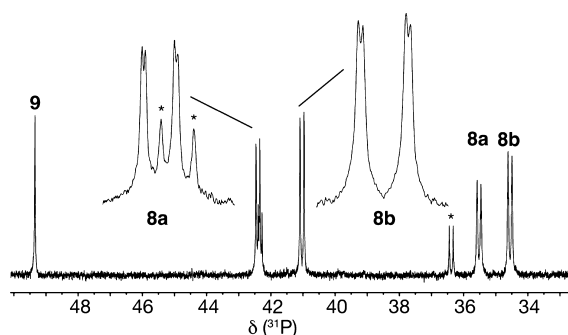


Figure 5. ^{31}P NMR signals of $[\text{RuCl}(^{15}\text{N-EDA})(\text{PNNP})]^+$ ($^{15}\text{N-8}$) (202 MHz, CD_2Cl_2 , $-80\text{ }^{\circ}\text{C}$) showing the P,N-coupling of 2 Hz (signals marked “*” belong to an unknown impurity).^{25,28}

$^{\circ}\text{C}$ shows, along with the signals of the *s-trans* and *s-cis* isomers of free, unreacted $^{15}\text{NNCHCO}_2\text{Et}$ at $\delta -7.6$ and -1.3 ,^{31b} two broad signals at $\delta -24.8$ and -25.3 that we assign to the rotamers of *trans*- $[\text{RuCl}(^{15}\text{N-EDA})(\text{PNNP})]^+$ ($^{15}\text{N-8}$) (Figure 6).³⁹

A broad triplet at $\delta -89.9$ is assigned to the $\text{Ru}-^{15}\text{NN}$ isomer of the above-mentioned dinitrogen complex *trans*- $[\text{RuCl}(\text{N}_2)(\text{PNNP})]^+$ (**9**). The 2J ($^{31}\text{P}, ^{15}\text{N}$) value of 2.3 Hz

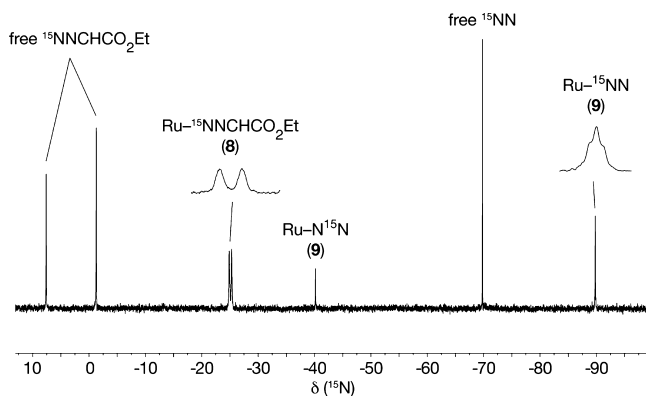


Figure 6. $^{15}\text{N}\{^1\text{H}\}$ NMR spectrum of the reaction solution of 4PF_6 , **5a** (1 equiv), and ^{15}N -EDA (10 equiv) at $-60\text{ }^{\circ}\text{C}$ (50.7 MHz, CD_2Cl_2).

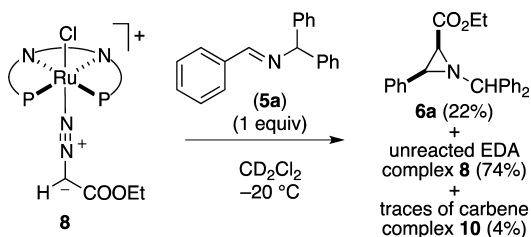
indicates that the two phosphorus atoms occupy *cis* positions to the dinitrogen ligand.^{38b} A signal at $\delta -40.2$, which is diagnostic of a $\text{Ru}-^{15}\text{N}$ moiety, suggests an equilibrium between the $\text{Ru}-^{15}\text{N}-\text{N}$ and the $\text{Ru}-\text{N}-^{15}\text{N}$ regioisomers and rules out the bridged *end-on/end-on* coordination.^{38b,40} This equilibrium possibly involves N_2 -dissociation from **9**, as the signal of free ^{15}NN in solution is visible at $\delta -71.0$.⁴¹ The low-temperature ^{31}P signal of **9** is a singlet (Figure 3) that broadens at higher temperatures, possibly because of the $\text{Ru}-^{15}\text{N}-\text{N}/\text{Ru}-\text{N}-^{15}\text{N}$ exchange. This multiplicity is apparently inconsistent with the suggested formulation *trans*- $[\text{RuCl}(\text{N}_2)(\text{PNNP})]^+$, but the two phosphines might be fortuitously isochronous, as the inequivalent P atoms of C_1 -symmetric *trans* Ru/PNNP complexes generally exhibit similar chemical shifts.¹⁹

In sum, the above experiments show that, when a CD_2Cl_2 solution of $[\text{RuCl}(\text{OEt}_2)(\text{PNNP})]\text{PF}_6$ (**4PF**₆) and imine **5a** (1 equiv) is treated with ^{13}C -EDA (or ^{15}N -EDA) in excess (10 equiv) at $-78\text{ }^{\circ}\text{C}$, the EDA complex *trans*- $[\text{RuCl}(\text{EDA})(\text{PNNP})]^+$ (**8**) is the major species in solution below $-20\text{ }^{\circ}\text{C}$. We have recently reinvestigated the behavior of $[\text{RuCl}(\text{OEt}_2)(\text{PNNP})]\text{PF}_6$ (**4PF**₆) in CD_2Cl_2 solution and found that it dissociates to give the five-coordinate complex **2** and Et_2O even below room temperature, whereas the aqua complex **3** is considerably more stable and less labile (Scheme 3).¹⁹ As the Et_2O adduct **4PF**₆ reacts with a stoichiometric amount of EDA to give **8** quantitatively even at $-78\text{ }^{\circ}\text{C}$, we conclude that *end-on*-bound EDA is a better ligand than Et_2O and is in agreement with the weak binding of Et_2O . The reactivity of the EDA complex **8** is discussed in the next paragraph.

Reaction of EDA Complex **8 with Imine **5a**.** Upon slowly raising the temperature of solutions containing the diazoester complex **8**, imine **5a**, and an excess of ^{13}C -EDA from $-78\text{ }^{\circ}\text{C}$, the imine is fully converted to aziridine **6a**, and the signals of free EDA disappear (see Supporting Information, experiment 3). After reaching room temperature, the diazoester complex **8** begins to decay to the carbene complex $^{13}\text{C-10}$ just after free $\text{N}_2^{13}\text{CHCO}_2\text{Et}$ is consumed completely (Figure S11 in the Supporting Information). The formation of $^{13}\text{C-10}$ is quantitative within 15 min. After 4 h, the *trans*-carbene complex $^{13}\text{C-10}$ is decomposed to the alkyl derivative $[\text{RuCl}(^{13}\text{CH}_2\text{CO}_2\text{Et})(\text{PNNP})]$ ($^{13}\text{C-11}$).⁴² The reaction between complex **4PF**₆, imine **5a**, and ^{13}C -EDA (1:1:10 ratio) in CD_2Cl_2 was repeated three times in the temperature range between -78 and $25\text{ }^{\circ}\text{C}$ with essentially the same results.

The above experiment was slightly modified to test whether aziridine **6a** is formed in the presence of EDA complex **8** after quantitative EDA consumption (see experiment 5 in the Supporting Information). Thus, a CD_2Cl_2 solution of the EDA complex $^{13}\text{C-8}$ (prepared as describe above) was warmed to $0\text{ }^{\circ}\text{C}$ in the NMR spectrometer until free $\text{N}_2^{13}\text{CHCO}_2\text{Et}$ was consumed. Then, the sample was cooled to $-78\text{ }^{\circ}\text{C}$, imine **5a** (1 equiv) was added thereto, and the sample temperature was increased in $20\text{ }^{\circ}\text{C}$ steps. At $-20\text{ }^{\circ}\text{C}$, a $(^{13}\text{C}, ^1\text{H})$ -HMQC experiment showed the signals of ^{13}C -labeled aziridine **6a** (22%), along with those of unreacted EDA complex **8** (74%) and a small amount (4%) of carbene complex **10** (Scheme 8). The facts that no free EDA is present in the solution under these conditions and that the dissociation of EDA complex **8** is slow on the NMR time scale below $0\text{ }^{\circ}\text{C}$ ⁴³ are a strong indication that the carbene is transferred to the imine from the EDA complex **8**.

Scheme 8

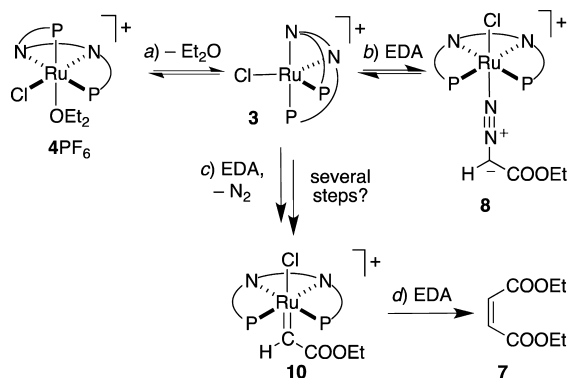


As the EDA complex **8** is competent for aziridine formation, the rate of its decay to the carbene complex **10** must affect the yield of aziridine, and hence the chemoselectivity of the reaction. The possible mechanism of the formation of carbene complex **10** and its involvement in the formation of diethyl maleate are discussed in the next paragraphs.

The Decay of EDA Complex 8. A key feature of the above results is that the outcome of the reaction of $[\text{RuCl}(\text{OEt}_2)(\text{PNNP})]^+$ (**4PF₆**) with EDA depends on the amount of EDA used. In fact, **4PF₆** reacts with a stoichiometric amount of EDA to give the carbene complex **10** at -78°C , whereas an excess of EDA (10 equiv) gives the diazoester complex **8** as the most abundant species in solution. At -78°C , only about 5% of EDA is converted to diethyl maleate (**7**) after 8 h, whereas substantial amounts of **7** (about 50%) are formed at -20°C during few minutes. However, the carbene complex **10** is formed in detectable amounts only after depletion of free EDA.

We explain the above observations on the basis of the reactions in Scheme 9. The Et_2O adduct **4PF₆**, in which the

Scheme 9



Et_2O ligand is weakly bound,¹⁹ possibly reacts with EDA with the intermediacy of the 16-electron complex **3a** (equilibrium a) to give either the *end-on* EDA complex **8** in a reversible fashion (path b) or irreversible N_2 extrusion to the carbene complex **10** (path c). When present in excess, EDA reacts with the carbene complex **10** to give diethyl maleate (**7**) (path d), and a further equivalent of EDA re-forms the diazoester complex **8**. This reaction sequence explains why the EDA complex **8** is the main species in solution in the presence of EDA in excess and why large amounts of carbene complex **10** are formed only after quantitative EDA consumption.

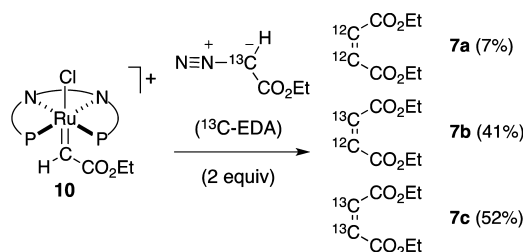
Overall, diazoalkane complexes are assumed to form the corresponding carbene complexes by dinitrogen extrusion, but the mechanistic details of this process are still not completely understood.^{34g,44,45} A crucial point for the decomposition to carbene is that an *end-on* diazoalkane complex of type **I** must isomerize to structure **V** (Chart 2) before N_2 extrusion can take

place. This has been originally proposed by Kodadek⁴⁶ and recently supported both by experiment⁴⁷ and by theory.⁴⁸ Calculations on $\text{Rh}(\text{I})/\text{PCP}$ complexes⁴⁴ have suggested that the **I–V** coordination modes of phenyldiazomethane may be close in energy. According to Milstein, the *end-on* complex **I** is not a true intermediate in the decomposition of the diazoalkane to carbene, but rather a resting state, and the diazoalkane dissociates and reattacks⁴⁹ the metal with the carbenoid C atom to give a $\sigma\text{-C}$ complex of type **V**, which then undergoes fast N_2 extrusion.^{34g,44,50}

An important consequence for the present discussion is that, to form the carbene complex **10**, the diazoester must dissociate from complex **8** and reattack the coordinatively unsaturated $[\text{RuCl}(\text{PNNP})]^+$ (**2**) with a different coordination mode. During this process, any donor present in solution (such as Et_2O or even the anion, see below) can intercept the 16-electron species **2** to form a coordinatively saturated complex that cannot react with EDA. The relevance of this point to the chemoselectivity of aziridine formation will be discussed below.

The Formation of Maleate. To prove its involvement in the formation of diethyl maleate, the nonlabeled carbene complex $[\text{RuCl}(\text{CHCO}_2\text{Et})(\text{PNNP})]^+$ (**10**), prepared from $[\text{RuCl}(\text{PNNP})]\text{PF}_6$ (**2**) and EDA in CD_2Cl_2 at room temperature,^{18a,51} was treated with ^{13}C -EDA (2 equiv) at -78°C . The $(^{13}\text{C},^1\text{H})$ -HMQC and ^1H NMR spectra recorded immediately after reinserting the sample into the spectrometer at -78°C showed the presence of the diazoester complex ^{13}C -**8**, of traces of the carbene complex $[\text{RuCl}(^{13}\text{C}\text{HCO}_2\text{Et})(\text{PNNP})]\text{PF}_6$ (^{13}C -**10**), and of different isotopomers of diethyl maleate, which were quantified by integration of the ^1H NMR spectrum (41% mono- ^{13}C -labeled **7b**, 52% doubly labeled **7c**, and 7% unlabeled **7a**) (Scheme 10).

Scheme 10



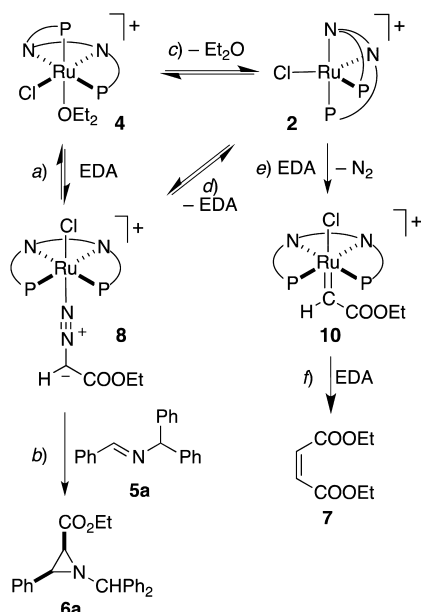
The formation of the monolabeled **7b** (41%) is diagnostic of the reaction of N_2 - $^{13}\text{C}\text{HCO}_2\text{Et}$ with unlabeled $[\text{RuCl}(\text{CHCO}_2\text{Et})(\text{PNNP})]^+$ (**10**), whereas 2,3-bis(^{13}C)-ethyl maleate (**7c**, 52%) is formed by successive carbene formation from ^{13}C -EDA. Accordingly, upon increasing the temperature, the ^{13}C -**10**:**10** ratio gradually increased as the nonlabeled carbene complex was consumed. Finally, we attribute the small amount of nonlabeled **7a** (7%) to residual ^{12}C in N_2 - $^{13}\text{C}\text{HCO}_2\text{Et}$, whose isotopic purity was 97%.

We conclude that the carbene complex **10**, besides being nonproductive in aziridination, is competent for the formation of diethyl maleate by reaction with the diazoalkane. Analogously, the carbene complex $[\text{Rh}(\text{CHPh})(\text{PCP})]^+$ (**PCP** is the tridentate pincer ligand 1,3-bis[(diisopropylphosphanyl)methyl]benzene) reacts with PhCHN_2 to give stilbene at -50°C , a temperature at which the decomposition of the diazoalkane complex to the corresponding carbene species is very slow.⁴⁴ Also $\text{Co}(\text{II})$ porphyrin carbene complexes react

with EDA to give diethyl maleate.^{26c} The selective formation of the *cis*-olefin (that is, maleate rather than fumarate) with the Ru/PNNP catalyst $4PF_6$ is consistent with the previously suggested mechanisms for the nucleophilic attack of aryldiazomethanes onto metal carbene complexes of Rh(II) and Cu(I).⁵²

A New Imine Aziridination Mechanism. The available evidence suggests that the Ru/PNNP-catalyzed imine aziridination follows the unprecedented path c of Scheme 1, whose key feature is the intermediacy of the *end-on* diazoester complex *trans*-[RuCl(EDA)(PNNP)]⁺ (8) (Scheme 11). In fact, the

Scheme 11



reactions discussed above show that complex 8, formed from the labile Et_2O adduct 4 or with the intermediacy of the 16-electron complex 2,¹⁹ (i) is the resting species of the catalyst during aziridination in the presence of an excess of EDA, (ii) reacts with the imine to give aziridine 6a and the dinitrogen complex 9 (reaction b), and (iii) decays to the carbene complex 10 after quantitative EDA consumption (reaction e). The latter reaction probably involves EDA dissociation from 8 and reattack of EDA to give the carbene complex 8 (reactions d, e).^{18a} Literature precedents suggest that the latter reaction may involve an undetected intermediate, possibly an EDA adduct with a different binding mode as discussed above (Chart 2).^{34g,44,46,47}

In the reactions on the left of Scheme 11, the EDA adduct 8 produces aziridine (reactions a and b), whereas the right branch leads to the formation of diethyl maleate (7) by the reaction of the carbene complex 10 with EDA (reaction f). This reaction has been observed even at $-78\text{ }^{\circ}\text{C}$ (see above) and is thus faster than carbene transfer from the EDA complex 8 to the imine. Therefore, the chemoselectivity toward aziridine is controlled by the rate of formation of carbene 10.

The coordinatively unsaturated complex 2 is the most reactive species in solution and most probably the common intermediate in the formation either of the EDA adduct 8 or of the carbene complex 10. Therefore, all factors that influence its concentration and reactivity in solution are expected to play a pivotal role in determining the chemoselectivity. We have previously reported that the equilibrium between the Et_2O

adduct $[RuCl(OEt_2)(PNNP)]^+$ (4) and the 16-electron complex $[RuCl(PNNP)]^+$ (2) (Scheme 11c) is fast on the NMR time scale at room temperature and is frozen out at $-40\text{ }^{\circ}\text{C}$.¹⁹ Therefore, we suggest that diethyl ether competes with EDA for coordination to the 16-electron complex 2 at the reaction temperature ($0\text{ }^{\circ}\text{C}$) and hence slows down the formation of the carbene complex 10 because the latter reaction requires the $\eta^2\text{-N}_2$ -coordination of EDA, which should be less favored than *end-on* coordination as in 8.⁴⁴ In agreement with the above interpretation, aziridine is formed also at room temperature with the aqua complex $[RuCl(OH_2)(PNNP)]PF_6$ (3),²⁰ because water binds to ruthenium more strongly than Et_2O and its dissociation is less favorable both thermodynamically and kinetically.¹⁹

The above line of reasoning would also explain the anion effect on the chemoselectivity (Table 1). Although the low-temperature studies were inconclusive (see above and Supporting Information), there is literature precedent for the ranking of the coordinating ability of so-called “noncoordinating” anions such as PF_6^- , BF_4^- , and SbF_6^- , which shows that BF_4^- and SbF_6^- are more coordinating than PF_6^- .²⁴ In the case of 4Y, we suggest that SbF_6^- and BF_4^- intercept the 16-electron complex $[RuCl(PNNP)]^+$ (2) more efficiently than PF_6^- , thus preventing the decay of EDA to carbene.⁵³ Overall, the above results suggest that any coordinating species present in solution (either neutral molecule or anion) improves the chemoselectivity toward aziridination, which opens the space for further improvement.

Why Are Ruthenium Carbenes Weak Electrophiles?

We have discussed above the role played by the EDA complex 8 and by the carbene complex 10 in the formation of aziridine. The question to be answered in this paragraph is why imine 5a reacts with the EDA complex 8 but not with carbene complex 10. The lack of reactivity of carbene complex 10 toward imines finds an interesting precedent in Che’s report of ruthenium porphyrin-catalyzed imine aziridination.²⁷ Also in that case, the carbene complex formed in situ from $[Ru(CO)(F_{20}\text{-TPP})]$ ($H_2(F_{20}\text{-TPP}) = \text{meso-tetrakis(pentafluorophenyl)porphyrin}$) failed to react with imines. In contrast, imine aziridination with copper(I)⁴ and rhodium(II)⁶ catalysts is thought to involve nucleophilic attack of the imine onto a carbene complex (Scheme 1a). Late transition metals are known to form carbene complexes that are particularly electrophilic.⁵⁴ An extremely simplified, but useful, explanation of the high electrophilicity of mononuclear⁵⁵ transition metal complexes is given in Figure 7, which sketches the π bond between the metal and the carbene ligand.

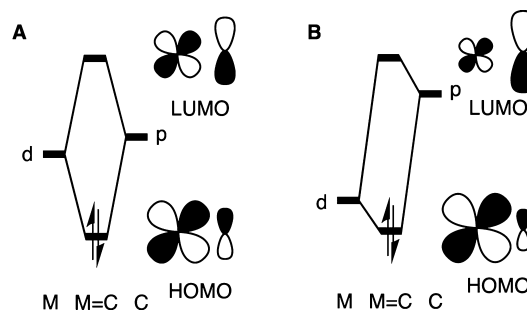
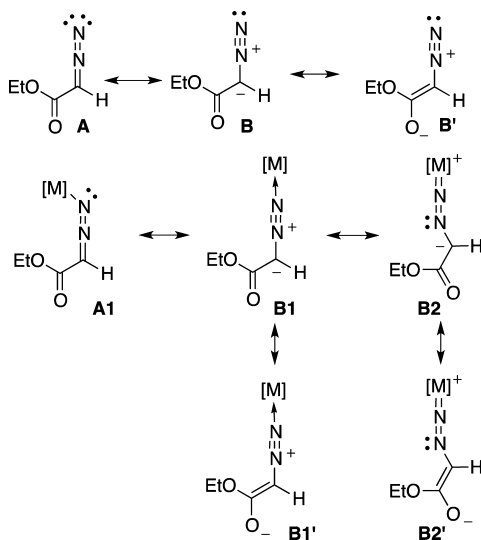


Figure 7. Qualitative sketch of form and energy of the π -M-C orbital in carbene complexes.

The energy of the metal d orbital sinks significantly below that of the p orbital of the carbenoid C atom upon changing the metal from ruthenium (case A) to a late transition metal such as copper (case B). Therefore, going on from A to B, the π -bonding MO increases its localization on the metal, whereas the empty π^* orbital shifts toward the carbene. As the latter orbital is the LUMO involved in a nucleophilic attack, carbene complexes of late transition metals tend to be more electrophilic than those of the elements to their left in the periodic table. Therefore, we suggest that the electrophilicity of ruthenium carbenes may be too low for azomethine ylide formation with imines, which are weak nucleophiles (Schemes 1a and 2). In the next paragraph, we discuss electronic arguments that support the alternative pathway c, in which the metal-bound diazoalkane acts as nucleophile toward the imine.

Reactivity of Diazoalkane Complexes. In linear (Ia) or singly bent (Ib) *end-on* diazoalkane complexes (Chart 2), the diazoalkane acts as a $2e^-$ σ -donor, but the bonding interaction is complemented, at least in principle, by a π -back-bonding contribution with late transition metals. Accordingly, the structure of *end-on* bound diazoesters is very sensitive to the electronic properties of the metal and to the substitution pattern of the carbenoid C atom. Complexes of type Ia contain a neutral diazoalkane ligand whose carbenoid atom has some sp^3 character,^{34a} which increases its carbanion character and hence its nucleophilicity. To understand this, it is useful to consider the total valence bond representation of non-coordinated EDA to which both structures A and B contribute. This is depicted in Chart 3, which shows the relevant canonical structures for free and coordinated EDA.

Chart 3



We recall that the chemical shift of the carbenoid C atom and the dynamic NMR spectroscopic behavior suggest a linear, *end-on* structure for the EDA complex **8**, which implies that the canonical structures **B1** and **B2** prevail over **A1**. The low rotation barrier around the $\text{EtO}_2\text{C}-\text{CHN}_2$ bond in **8** as compared to free EDA (Figure 1) indicates that the contribution of the canonical structures of type **B** to resonance increases upon coordination at the cost of structures of types **A** and **B'**. We conclude that, in coordinated EDA, the canonical structures **B1** and **B2**, in which the carbenoid C atom is mostly sp^3 and bears a formal negative charge, give a larger

contribution to the resonance hybrid than in free EDA, thus accounting for the increased nucleophilicity of the former.

A qualitative MO-LCAO analysis of the π -back-donation from the d^6 metal ion reinforces this line of reasoning. The HOMO of free diazomethane is a nonbonding orbital of π -symmetry that is substantially localized on the carbon atom (Figure 8, left).⁵⁶ In the linear diazoalkane complexes (**B** and

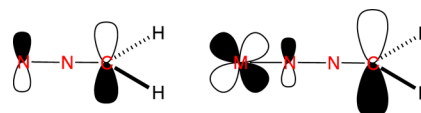


Figure 8. Qualitative sketch of the HOMO of free (left) and metal-bound (right) CH_2N_2 .

B', Chart 3), the 4-electron π - π repulsion⁵⁷ with the fully occupied d orbitals of π -symmetry of the octahedral d^6 metal ion destabilizes the HOMO of the CH_2N_2 ligand and rehybridizes it toward the carbenoid C atom (Figure 8, right), thus increasing its nucleophilic character.⁵⁸ In agreement with the suggestion that the coordination to an electron-rich late-transition metal enhances the nucleophilicity of diazoalkanes, Lebel has claimed that the $[\text{RhCl}(\text{PPh}_3)_3]$ -catalyzed methylenation of aldehydes with trimethylsilyldiazomethane involves an *end-on* linear TMSCHN_2 complex⁵⁹ whose carbenoid C atom undergoes protonation by 2-propanol and other alcohols.⁶⁰

Also, diazoalkanes are believed to behave as nucleophiles toward imines in acid-catalyzed aziridination^{12c} and in 1,3-dipolar cycloaddition⁶¹ reactions. The frontier orbital (FO) energies calculated for ethyl diazoacetate (HOMO: -9.75 eV)⁶² and *N*-methylbenzaldimine (LUMO 3.0 eV),⁶³ which can be taken as model for **5a**, show a FO gap of 12.75 eV (Figure 9). Both in the Brønsted acid-catalyzed aza-Darzens reac-

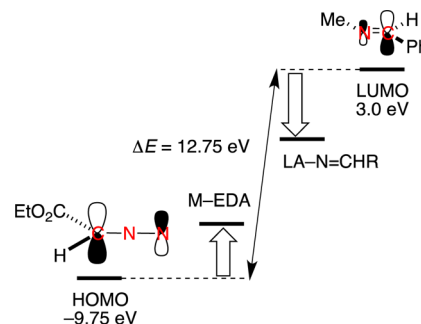


Figure 9. Effect of coordination on the energies of the frontier orbitals involved in carbene transfer from EDA to imine.

tion^{13–15} and with Lewis acidic catalysts,^{11,12} this gap is reduced because the acid stabilizes the LUMO of the imine. In the case of the ruthenium-catalyzed aziridination, we suggest that the FO gap is reduced because the coordination to a metal with filled π -orbitals destabilizes the HOMO of the diazoester (as discussed above), which promotes the nucleophilic attack of the carbenoid C atom of EDA to the free, nonactivated imine.

As the HOMO of the diazoester and the LUMO of the imine are mainly localized on the respective C atoms, the formation of the C–C bond should play a major role in both cases. Accordingly, it is broadly accepted that the first step of acid-catalyzed imine aziridination is the attack of the diazoalkane onto the C–N π -bond to give a α -diazonium- β -amino ester

that collapses to the aziridine by intramolecular, S_N2 -like attack of the azomethine nitrogen onto the carbenoid C atom.^{15a} In the case of the EDA adduct **8**, the elimination of N_2 is assisted by the formation of the dinitrogen complex *trans*-[RuCl(N_2)-(PNNP)]⁺ (**9**) (Scheme 11).⁶⁴

The observation of the dinitrogen complex **9** is enlightening for a further reason. As N_2 is weaker both as σ -donor and as π -acceptor than the isoelectronic CO ligand,⁶⁵ only a few ruthenium complexes meet the requirements for the formation of dinitrogen complexes, which are the presence of a ligand with low *trans* influence (Cl or N) in the *trans* position (to avoid competition with N_2) and of strong σ -donors (aryl, alkynyl, or alkyl phosphines) to enhance the electron density at the metal and hence π -back-bonding to N_2 . Both conditions are fulfilled for some recently reported dinitrogen complexes of ruthenium(II) with a PCP,⁶⁶ PNP,⁶⁷ POP,⁶⁸ P_2N_2 ,⁶⁹ or P_4 ⁷⁰ donor set. In *trans*-[RuCl(N_2)(PNNP)]⁺ (**9**), N_2 is *trans* to the chloro ligand, which has a small *trans* influence. On the other hand, the formation of **9** suggests that, despite the positive charge of the complex and the presence of aryl (rather than alkyl) phosphines, the π -back-donating ability of the [RuCl-(PNNP)]⁺ fragment is significant, which plays a key role in the activation of EDA as discussed above.

Conclusion and Outlook. Ruthenium/PNNP catalysts give the highest enantioselectivity ever observed in the transition metal-catalyzed aziridination of imine with diazoesters. We suggest that the reaction mechanism implies carbene transfer from an intermediate diazoalkane complex rather than from a carbene complex. The fundamental difference with Cu- and Rh-based catalysts is that no azomethine ylide is formed, whose dissociation from the chiral catalyst has been held responsible for the low enantioselectivity observed with late transition metal catalysts. The disclosure of this unprecedented mechanism generates new hope in the endeavor of developing highly enantioselective imine aziridination catalysts based on transition metals that may complement those based on chiral acids. Our next goal is to produce further evidence for the suggested mechanism and to gather fundamental understanding of the factors that govern the decay of the diazoalkane adduct to the carbene complex and the mechanism of enantioselection, which is necessary to improve the chemoselectivity toward aziridine formation.

EXPERIMENTAL SECTION

General. Reactions with air- or moisture-sensitive materials were carried out under an argon atmosphere using Schlenk techniques. All solvents were distilled from an appropriate drying agent under argon prior to use (CH_2Cl_2 and CD_2Cl_2 from CaH_2 , hexane from Na/benzophenone, diethyl ether from Na/phthalic acid ethyl ester). [RuCl₂(PPh₃)₃] and [RuCl₂(PNNP)] (**1**) (PNNP = *N,N'*-bis(*o*-(diphenylphosphino)benzylidene)-(1*S*,2*S*)-diaminocyclohexane) were prepared as reported.^{71,72} Commercial (1*S*,2*S*)-*N,N'*-bis(2-bromobenzylidene)cyclohexane-1,2-diamine, (Et₃O)PF₆, and (Et₃O)-BF₄ (stabilized with 3–5% diethyl ether) were used without further purification. Triethyloxonium hexafluoroantimonate was prepared by a literature procedure by using silver hexafluoroantimonate instead of silver tetrafluoroborate.⁷³ Isotopically labeled $N_2^{13}CHCO_2Et$ and $^{15}NNCHCO_2Et$ were prepared according to a published procedure (see Supporting Information).⁷⁴ Imines were obtained from the corresponding amines by condensation reactions. For NMR spectra, ¹H and ¹³C positive chemical shifts δ (in ppm) are downfield from tetramethylsilane, and are referenced to the residual solvent signal. Mass spectra were measured by the MS service of the Laboratorium für Organische Chemie (ETH Zürich). Optical rotations were measured in a thermostated 1 dm cell (20 °C). Elemental analyses

were carried out by the Laboratory of Microelemental Analysis (ETH Zürich). Enantiomeric excesses were determined by chiral HPLC (IB column, 3 μ m) equipped with a DAD detector to check peak purity.

Standard Catalytic Run with **4Y.** In the optimized protocol (see Supporting Information, Table S1), the catalyst was prepared by stirring a CH_2Cl_2 solution (3 mL) of [RuCl₂(PNNP)] (**1**) (0.0482 mmol, 0.1 equiv) and (Et₃O)Y (0.0482 mmol, 0.1 equiv) at room temperature overnight, upon which the color changed from red to brown. Then, the imine (0.49 mmol, 1 equiv) was added, and the resulting solution was cooled down to 0 °C. Ethyl 2-diazoacetate (EDA) (0.48 mmol, 1 equiv, or 1.92 mmol, 4 equiv, neat) was added in one portion, and the reaction solution was stirred for 24 h at 0 °C. Then, a known amount of 2,4,6-trimethoxybenzene was added as internal standard to the crude mixture, and the conversion of the imine (**5**) and the yield of crude *cis*- and *trans*-aziridines (**6**) were determined by ¹H NMR spectroscopy. The oily residue was subjected to flash chromatography on silica (hexane/ethyl acetate 95:5) to give a white crystalline solid, which consisted exclusively of *cis*-aziridine. The enantiomeric excess of *cis*-**6** was determined by chiral HPLC analysis (see Supporting Information).

ASSOCIATED CONTENT

Supporting Information

Details of NMR spectroscopic studies, experimental details of catalytic reactions, and product characterization data. This material is available free of charge via the Internet at <http://pubs.acs.org>.

AUTHOR INFORMATION

Corresponding Author

*E-mail: mezzetti@inorg.chem-ethz.ch.

Notes

The authors declare no competing financial interest.

ACKNOWLEDGMENTS

The authors are grateful to the Swiss National Science Foundation for financial support (Grant No. 2-77767-10).

REFERENCES

- (1) (a) Michaux, J.; Niel, G.; Campagne, J. M. *Chem. Soc. Rev.* **2009**, 38, 2093. (b) Sweeney, J. B. *Chem. Soc. Rev.* **2002**, 31, 247. (c) McCoull, W.; Davis, F. A. *Synthesis* **2000**, 1347. (d) Hu, X. E. *Tetrahedron* **2004**, 60, 2701.
- (2) Moessner, C.; Bolm, C. *Catalyzed Asymmetric Aziridinations. In Transition Metals for Organic Synthesis*, 2nd ed.; Beller, M., Bolm, C., Eds.; Wiley-VCH: Weinheim, DE, 2004; Vol. 2, pp 389–402.
- (3) (a) Pellissier, H. *Tetrahedron* **2010**, 66, 1509. (b) Friestad, G. K.; Mathies, A. K. *Tetrahedron* **2007**, 63, 2541. (c) Müller, P.; Fruit, C. *Chem. Rev.* **2003**, 103, 2905.
- (4) Hansen, K. B.; Finney, N. S.; Jacobsen, E. N. *Angew. Chem., Int. Ed.* **1995**, 34, 676.
- (5) Bartnik, R.; Mloston, G. *Tetrahedron* **1984**, 40, 2569.
- (6) Moran, M.; Bernardinelli, G.; Müller, P. *Helv. Chim. Acta* **1995**, 78, 2048.
- (7) (a) Juhl, K.; Hazell, R. G.; Jorgensen, K. A. *J. Chem. Soc., Perkin Trans. 1* **1999**, 2293. See also: (b) Redlich, M.; Hossain, M. M. *Tetrahedron Lett.* **2004**, 45, 8987.
- (8) (a) Aggarwal, V. K.; Thompson, A.; Jones, R. V. H.; Standen, M. C. H. *J. Org. Chem.* **1996**, 61, 8368. (b) Aggarwal, V. K.; Vasse, J. L. *Org. Lett.* **2003**, 5, 3987. (c) Aggarwal, V. K.; Winn, C. L. *Acc. Chem. Res.* **2004**, 37, 611.
- (9) (a) Evans, D. A.; Faul, M. M.; Bilodeau, M. T.; Anderson, B. A.; Barnes, D. M. *J. Am. Chem. Soc.* **1993**, 115, 5328. (b) Li, Z.; Quan, R. W.; Jacobsen, E. N. *J. Am. Chem. Soc.* **1995**, 117, 5889.
- (10) Kawabata, H.; Omura, K.; Uchida, T.; Katsuki, T. *Chem. Asian J.* **2007**, 2, 248.

- (11) Casarrubios, L.; Perez, J. A.; Brookhart, M.; Templeton, J. L. *J. Org. Chem.* **1996**, *61*, 8358.
- (12) Account article: (a) Zhang, Y.; Lu, Z.; Wulff, W. D. *Synlett* **2009**, 2715. Selected papers: (b) Hu, G.; Huang, L.; Huang, R. H.; Wulff, W. D. *J. Am. Chem. Soc.* **2009**, *131*, 15615. (c) Hu, G.; Gupta, A. K.; Huang, R. H.; Mukherjee, M.; Wulff, W. D. *J. Am. Chem. Soc.* **2010**, *132*, 14669. (d) Desai, A. A.; Wulff, W. D. *J. Am. Chem. Soc.* **2010**, *132*, 13100. (e) Veticatt, M. J.; Desai, A. A.; Wulff, W. D. *J. Am. Chem. Soc.* **2010**, *132*, 13104. (f) Gupta, A. K.; Mukherjee, M.; Wulff, W. D. *Org. Lett.* **2011**, *13*, 5866. Seminal paper: (g) Antilla, J. C.; Wulff, W. D. *J. Am. Chem. Soc.* **1999**, *121*, S099.
- (13) (a) Hashimoto, T.; Uchiyama, N.; Maruoka, K. *J. Am. Chem. Soc.* **2008**, *130*, 14380. (b) Hashimoto, T.; Nakatsu, H.; Yamamoto, K.; Maruoka, K. *J. Am. Chem. Soc.* **2011**, *133*, 9730. (c) Hashimoto, T.; Nakatsu, H.; Yamamoto, K.; Watanabe, S.; Maruoka, K. *Chem. Asian J.* **2011**, *6*, 607.
- (14) Selected aza-Darzens reactions catalyzed by chiral phosphoric acids: (a) Akiyama, T.; Suzuki, T.; Mori, K. *Org. Lett.* **2009**, *11*, 2445. (b) Zeng, X.; Zeng, X.; Xu, Z.; Lu, M.; Zhong, G. *Org. Lett.* **2009**, *11*, 3036.
- (15) (a) Review article: Johnston, J. N.; Muchalski, H.; Troyer, T. L. *Angew. Chem., Int. Ed.* **2010**, *49*, 2290. (b) Mechanistic studies: Troyer, T. L.; Muchalski, H.; Hong, K. B.; Johnston, J. N. *Org. Lett.* **2011**, *13*, 1790.
- (16) For the first synthesis of **2a**, see: Gao, J. X.; Ikariya, T.; Noyori, R. *Organometallics* **1996**, *15*, 1087.
- (17) Account articles on Ru/PNNP catalysts: (a) Mezzetti, A. *Dalton Trans.* **2010**, 7851. (b) Bonaccorsi, C.; Mezzetti, A. *Curr. Org. Chem.* **2006**, *10*, 225.
- (18) (a) Bachmann, S.; Furler, M.; Mezzetti, A. *Organometallics* **2001**, *20*, 2102. (b) Bonaccorsi, C.; Bachmann, S.; Mezzetti, A. *Tetrahedron: Asymmetry* **2003**, *14*, 845. (c) Bonaccorsi, C.; Mezzetti, A. *Organometallics* **2005**, *24*, 4953.
- (19) Schotes, C.; Ranocchiari, M.; Mezzetti, A. *Organometallics* **2011**, *30*, 3596.
- (20) Ranocchiari, M.; Mezzetti, A. *Organometallics* **2009**, *28*, 3611.
- (21) In the previously reported procedure,²⁰ EDA (1 or 4 equiv vs 4PF₆) was added (neat) in one portion to a cooled (−78 °C) CH₂Cl₂ solution (3 mL) containing **5a** (0.48 mmol) and the catalyst 4PF₆ (10 mol%) (prepared by activation of [RuCl₂(PNNP)] (**1**) (0.048 mmol) with (Et₃O)PF₆ (1 equiv) overnight), followed by rapid heating to room temperature.
- (22) The yield of crude aziridine is given as the sum of the *cis* and *trans* isomers as obtained by integration of the ¹H NMR spectrum of the crude reaction mixture after addition of 1,3,5-trimethoxybenzene as internal standard.
- (23) The fate of the small amounts of *trans*-**6a** was assessed by performing a catalytic run under the conditions of Table S1, entry 4 (see Supporting Information), but with a 2-fold amount of catalyst, imine, EDA, and solvent. Under the standard workup conditions (flash chromatography over silica with hexane/ethyl acetate in 95:5 ratio), *trans*-**6a** was detected in the fractions containing the unreacted imine **5a**.
- (24) (a) Although there is no general consensus concerning the relative coordinating ability of PF₆[−], BF₄[−], and SbF₆[−], PF₆[−] is considered to be the least coordinating anion in these series, see: (b) Beck, W.; Sünkel, K. *Chem. Rev.* **1998**, *88*, 1405. (c) Honeychuck, R. V.; Hersh, W. H. *Inorg. Chem.* **1989**, *28*, 2869.
- (25) A further byproduct is an unknown species (14%) that features an AX pattern at δ 42.3 and 36.3 (²J_{P,P'} = 24.8 Hz) (see Supporting Information, experiment 1, Figure S5, and footnote 28).
- (26) (a) Zhang, L. R.; Chan, K. S. *Organometallics* **2007**, *26*, 679. (b) Lu, H. J.; Dzik, W. I.; Xu, X.; Wojtas, L.; de Bruin, B.; Zhang, X. P. *J. Am. Chem. Soc.* **2011**, *133*, 8518. See also: (c) Penoni, Wanke, R.; Tollari, S.; Gallo, E.; Musella, D.; Ragaini, F.; Demartin, F.; Cenini, S. *Eur. J. Inorg. Chem.* **2003**, 1452.
- (27) Li, Y.; Chan, P. W. H.; Zhu, N. Y.; Che, C. M.; Kwong, H. L. *Organometallics* **2004**, *23*, 54.
- (28) The only other significant signal is the already observed unknown impurity featuring an AX pattern at δ 42.3 and 36.3 (²J_{P,P'} = 24.8 Hz) (Figure S7 in the Supporting Information) of an unknown product (13%), which cannot be either the imine complex [RuCl(**5a**)(PNNP)]⁺, as it is formed also in the reaction of the ether complex 4PF₆ with EDA, in which no imine is present (see Supporting Information, experiment 2, and footnote 25), or a carbenoid of any kind or a different isomer of the carbene complex **10**, as the present reaction does not involve the addition of EDA.
- (29) The ³¹P NMR spectrum of the reaction mixture at −78 °C showed that complex 4PF₆ was quantitatively converted to a mixture of products that encompass the dinitrogen complex **9** (13%) and several unknown species.
- (30) The ¹H NMR CHCO₂Et signal of free EDA is split by the coupling to ¹³C (¹J_{C,H} = 205 Hz) (see Supporting Information, experiment 3, Figure S8). The signals of the carbene complex ¹³C-**9**, ¹³C-maleate, and of an unknown ¹³C-containing species were present in traces (2–3% of ¹³C-EDA). The latter species must be closely related to EDA because of its J_{C,H} value, which is comparable to the ones of N₂¹³CHCO₂Et (Figure S8 in the Supporting Information). This signal disappeared upon heating to −20 °C and was never observed at higher temperatures.
- (31) (a) Kaplan, F.; Meloy, G. K. *J. Am. Chem. Soc.* **1966**, *88*, 950. (b) Lichter, R. L.; Srinivasan, P. R.; Smith, A. B.; Dieter, R. K.; Denny, C. T.; Schulman, J. M. *J. Chem. Soc., Chem. Commun.* **1977**, 366.
- (32) Gao, Y.; Jennings, M. C.; Puddephatt, R. J.; Jenkins, H. A. *Organometallics* **2001**, *20*, 3500.
- (33) The *trans* configuration is indicated by a (³¹P,¹H)-HMQC spectrum of **8** at −60 °C (Figure S10 in the Supporting Information) that shows a ⁴J_{P,H} coupling constant of about 18 Hz for both imine H atoms (despite their signals being overlapped with those of the other Ru/PNNP complexes in solution). This is diagnostic of two *trans*-P–Ru–N moieties and hence of the *trans* configuration (see ref 19 for a discussion).
- (34) (a) Dartiguenave, M.; Menu, M. J.; Deydier, M.; Dartiguenave, Y.; Siebald, H. *Coord. Chem. Rev.* **1998**, *178*, 623. See also: (b) Mizobe, Y.; Ishii, Y.; Hidai, M. *Coord. Chem. Rev.* **1995**, *139*, 281. Selected examples: (c) Brandt, L.; Wolf, J.; Werner, H. *J. Organomet. Chem.* **1993**, *444*, 235. (d) Werner, H.; Schneider, M. E.; Bosch, M.; Wolf, J.; Teuben, J. H.; Meetsma, A.; Troyanov, S. I. *Chem.—Eur. J.* **2000**, *6*, 3052. (e) Ortmann, D. A.; Weberndörfer, B.; Ilg, K.; Laubender, M.; Werner, H. *Organometallics* **2002**, *21*, 2369. (f) Werner, H.; Mahr, N.; Wolf, J.; Fries, A.; Laubender, M.; Bleuel, E.; Garde, R.; Lahuerta, P. *Organometallics* **2003**, *22*, 3566. (g) Zhang, J.; Gandelman, M.; Shimon, L. J. W.; Milstein, D. *Organometallics* **2008**, *27*, 3526. (h) Dias, E. L.; Brookhart, M.; White, P. S. *J. Am. Chem. Soc.* **2001**, *123*, 2442.
- (35) We did not assign signals **8a** and **8b** to a particular isomer, whereas the assignment of the ³¹P NMR signal at δ 49.2 (at −60 °C) to a dinitrogen complex such as **9** is supported by the results of reaction with ¹⁵NNCHCO₂Et (see below).
- (36) The bending of N–N–C angle is diagnostic of some extent of π-back-bonding from the metal to the diazoalkane ligand.^{36a,b} (a) Schramm, K. D.; Ibers, J. A. *Inorg. Chem.* **1980**, *19*, 1231. (b) Herrmann, W. A.; Kriechbaum, G.; Ziegler, M. L.; Wulknitz, P. *Chem. Ber.* **1981**, *114*, 276. For further examples of linear or singly bent N–N–C diazoalkane complexes of d⁶ metal ions, see refs 34c–f and: (c) Schramm, K. D.; Ibers, J. A. *Inorg. Chem.* **1977**, *16*, 3287. (d) Menu, M. J.; Crocco, G.; Dartiguenave, M.; Dartiguenave, Y.; Bertrand, G. *J. Chem. Soc., Chem. Commun.* **1988**, 1598. (e) Bart, S. C.; Bowman, A. C.; Lobkovsky, E.; Chirik, P. J. *J. Am. Chem. Soc.* **2007**, *129*, 7212. (f) Albertin, G.; Antoniutti, S.; Baldan, D.; Castro, J.; Comparin, G. *Organometallics* **2013**, *32* (11), 3157–3160.
- (37) (a) Additionally, both neutral^{37b} and cationic^{37c} d⁶ diazoester complexes of osmium(II) are known, but have not been characterized structurally: (b) Werner, H.; Stüer, W.; Wolf, J.; Laubender, M.; Weberndörfer, B.; Herbst-Irmer, R.; Lehmann, C. *Eur. J. Inorg. Chem.* **1999**, 1889. (c) Albertin, G.; Antoniutti, S.; Bordignon, E.; Carrera, B. *Inorg. Chem.* **2000**, *39*, 4646.

- (38) (a) The ^{31}P , ^{15}N coupling was not resolved at -60°C , probably owing to the *s-cis/s-trans* equilibration process (Scheme 6) (see Supporting Information, experiment 4). The $^2J(^{31}\text{P}, ^{15}\text{N})$ value of ca. 2 Hz is diagnostic of a *cis* arrangement of the phosphine and EDA ligands.^{38b} The $(^{31}\text{P}, ^1\text{H})$ -HMQC spectrum shows a cross peak between the ^1H NMR signal (2 H) of the imine protons of the PNNP ligand and the phosphines, which is diagnostic of a *trans* stereochemistry for the N_2 complex **9**, as discussed above for the EDA complex ^{13}C -**8**.³³ (b) Donovan-Mtunzi, S.; Richards, R. L.; Mason, J. J. *Chem. Soc., Dalton Trans.* **1984**, 469.
- (39) The signals of **8** are broadened because of the lower barrier to rotation in the complex as compared to free EDA, see Results and Discussion.
- (40) Field, L. D.; Hazary, N.; Li, H. L.; Luck, I. J. *Magn. Reson. Chem.* **2003**, *41*, 709.
- (41) In previous experiments,^{18a,c} we have observed the broad ^{31}P NMR signal at δ ca. 49 of the dinitrogen complex **9**, but we incorrectly assigned it to *trans*- $[\text{RuCl}_2(\text{PNNP})]$ (**1**), which resonates at δ 48.0 in CDCl_3 .¹⁶ Clearly, the use of $^{15}\text{NNCHCO}_2\text{Et}$ was pivotal to assess the identity of **9**.
- (42) After 10 h at 20°C , the ^{31}P NMR spectrum of the reaction mixture shows the signals of the dinitrogen complex **9** (55%) and of the alkyl complex $[\text{RuCl}(\text{CH}_2\text{CO}_2\text{Et})(\text{PNNP})]$ (^{13}C -**11**) (45%). The latter signal is the AB part of an ABX system, where X is ^{13}C (Figure S12 in the Supporting Information). The alkyl complex ^{13}C -**11** is the main species in solution after 3 days at room temperature.
- (43) In a separate experiment in which the ^{13}C NMR signal at δ 58.0 of the ^{13}C -EDA ligand of **8** was irradiated in the presence of free ^{13}C -EDA at 0°C , no effect on the intensity of the latter signal was observed, which indicates that the exchange between free and coordinated EDA is slow at 0°C .
- (44) Cohen, R.; Rybtchinski, B.; Gandelman, M.; Rozenberg, H.; Martin, J. M. L.; Milstein, D. J. *Am. Chem. Soc.* **2003**, *125*, 6532.
- (45) (a) Werner, H.; Schwab, P.; Bleuel, E.; Mahr, N.; Steinert, P.; Wolf, J. *Chem.—Eur. J.* **1997**, *3*, 1375. (b) Wolf, J.; Brandt, L.; Fries, A.; Werner, H. *Angew. Chem., Int. Ed. Engl.* **1990**, *29*, 510.
- (46) (a) Maxwell, J. L.; Brown, K. C.; Bartley, D. W.; Kodadek, T. *Science* **1992**, *256*, 1544.
- (47) Wong, F. M.; Wang, J.; Hengge, A. C.; Wu, W. *Org. Lett.* **2007**, *9*, 1663 and references therein.
- (48) (a) Nowlan, D. T.; Gregg, T. M.; Davies, H. M. L.; Singleton, D. A. *J. Am. Chem. Soc.* **2003**, *125*, 15902. (b) Dzik, W. I.; Xu, X.; Zhang, X. P.; Reek, J. N. H.; de Bruin, B. J. *Am. Chem. Soc.* **2010**, *132*, 10891.
- (49) Accordingly, an excess of EDA inhibits the formation of carbene complex **10**, as it prevents the dissociation of **8** (besides scavenging the carbene complex **9** to give diethyl maleate (**7**)). In the experiments with the Et_2O adduct 4PF_6 , we did not observe any signal that may be assigned to EDA coordination of type **V**.
- (50) These calculations have also shown that bulky ligands hinder intramolecular isomerization along the pathway **I** \rightarrow **II** \rightarrow **III** \rightarrow **IV** (or **I** \rightarrow **II** \rightarrow **IV** \rightarrow **V**), hence hindering diazoalkane decomposition to carbene.
- (51) The low-temperature ^{31}P and ^1H NMR spectra of the reaction solution indicate the formation of the carbene species $[\text{RuCl}(\text{CHCO}_2\text{Et})(\text{PNNP})]^+$ (**10**) (84%) and of the dinitrogen complex **9** (16%) (Figure S15 in the Supporting Information).
- (52) (a) Oshima, T.; Nagai, T. *Tetrahedron Lett.* **1980**, *21*, 1251. (b) Ravi Shankar, B. K.; Shechter, H. *Tetrahedron Lett.* **1982**, *23*, 2277.
- (53) At this stage, we have no rationale for the effect of the anion on the enantioselectivity. However, we have previously observed a beneficial effect of SbF_6^- on the enantioselectivity of the asymmetric cyclopropanation of olefins catalyzed by $[\text{RuCl}_2(\text{PNNP})]$ after activation with AgSbF_6 .^{18c}
- (54) Nugent, W. A.; Mayer, J. M. In *Metal-Ligand Multiple Bonds*; Wiley: New York, USA, 1988; pp 28–29.
- (55) A different explanation must be considered for dimeric Rh(II) complexes, which form superelectrophilic carbene complexes via a 3-center/4-electron $\text{M}–\text{M}–\text{C}$ bond: Berry, J. F. *Dalton Trans.* **2012**, *41*, 700.
- (56) (a) Fleming, I. *Molecular Orbitals and Organic Chemical Reactions*, reference ed.; Wiley-VCH: Weinheim, 2010; p 325. (b) Jorgensen, W. L.; Salem, L. *The Organic Chemist's Book of Orbitals*; Academic Press: New York, 1973; p 127.
- (57) Caulton, K. G. *New J. Chem.* **1994**, *18*, 25.
- (58) As the binding to a Lewis acidic cationic complex is expected to decrease the electrophilicity of the ligand, the overall effect of the coordination of a diazoalkane to a transition metal complex discussed here is counterintuitive. However, it should be noticed that diazoalkanes use an energetically low-lying orbital for the σ -bond to the metal, whereas the HOMO has π -character with respect to the metal–diazoalkane bond and its energy primarily responds to π -effects. Also, the presence of a π -donating⁵⁷ chloro ligand *trans* to EDA in complex **8** enhances the π -back-bonding from ruthenium to the EDA ligand and hence increases its nucleophilicity.
- (59) For the preparation and X-ray study of a similar complex, see ref 34h.
- (60) (a) Lebel, H.; Paquet, V. *J. Am. Chem. Soc.* **2004**, *126*, 320. Interestingly, Wilkinson's catalyst $[\text{RhCl}(\text{PPh}_3)_3]$ was found to be more active in this reaction than the isoelectronic Ru(0) analogue $[\text{RuCl}(\text{NO})(\text{PPh}_3)_2]$. A possible explanation based on the above arguments is that NO^+ , a very strong π -accepting ligand, competes for the electron density on ruthenium and reduces the π -back-donation to the diazoalkane and, thus, its nucleophilic character.^{60b} (b) Lebel, H.; Paquet, V. *Organometallics* **2004**, *23*, 1187.
- (61) Review article: (a) Huisgen, R. *J. Org. Chem.* **1976**, *41*, 403. (b) Bastide, J.; Henri-Rousseau, O.; Aspart-Paccot, L. *Tetrahedron* **1974**, *30*, 3355.
- (62) Cheung, K. W. J.; Reynisson, J.; McDonald, E. *Tetrahedron Lett.* **2010**, *51*, 5915.
- (63) (a) This value^{63b} is more in keeping with the LUMO energy of 4.2 eV calculated for methyleneimine^{63c} than an alternative suggestion (-0.21 eV).^{63d} (b) Dal Colle, M.; Distefano, G.; Jones, D.; Guerrino, A.; Seconi, G.; Modelli, A. *J. Chem. Soc., Perkin Trans. 194*, 789. (c) See ref 56b, p 83. (d) Lerestif, J. M.; Perrocheau, J.; Tonnard, F.; Bazureau, J. P.; Hamelin, J. *Tetrahedron* **1995**, *51*, 6757.
- (64) Further studies will be directed to assess the stereochemistry of the approach between imine and diazoester, which can occur either in a transoid, antiperiplanar or in a cisoid, quasi $[2 + 3]$ fashion.^{12e}
- (65) Que, L.; Tolman, W. B. *Comprehensive Coordination Chemistry II*; Pergamon: Oxford, 2003; Vol. 8.
- (66) Zhang, J.; Barakat, K. A.; Cundari, T. R.; Gunnoe, T. B.; Boyle, P. D.; Petersen, J. L.; Day, C. S. *Inorg. Chem.* **2005**, *44*, 8379.
- (67) (a) Zhang, J.; Gandelman, M.; Shimon, L. J. W.; Rozenberg, H.; Milstein, D. *Organometallics* **2004**, *23*, 4026. (b) Amoroso, D.; Jabri, A.; Yap, G. P. A.; Gusev, D. G.; dos Santos, E. N.; Fogg, D. E. *Organometallics* **2004**, *23*, 4047.
- (68) Major, Q.; Lough, A. J.; Gusev, D. D. *Organometallics* **2005**, *24*, 2492.
- (69) Adams, C. J.; Bowen, L. E.; Humphrey, M. G.; Morrall, J. P. L.; Samoc, M.; Yellowlees, L. J. *Dalton Trans.* **2004**, 4130.
- (70) (a) Field, L. D.; Guest, R. W.; Vuong, K. Q.; Dalgarno, S. J.; Jensen, P. *Inorg. Chem.* **2009**, *48*, 2246. (b) Takei, I.; Nishibayashi, Y.; Ishii, Y.; Mizobe, Y.; Uemura, S.; Hidai, M. *J. Organomet. Chem.* **2003**, *679*, 32.
- (71) Hallman, P. S.; Stephenson, T. A.; Wilkinson, G. *Inorg. Synth.* **1970**, *12*, 237.
- (72) Gao, J. X.; Ikariya, T.; Noyori, R. *Organometallics* **1996**, *15*, 1087.
- (73) Hederich, V.; Wunderlich, K. *Arch. Pharm.* **1958**, *291*, 541.
- (74) Searle, N. E. *Org. Synth.* **1963**, Collect. Vol. 4, 424.